Electronic Supplementary Material (ESI) for Journal of Materials Chemistry C

Supporting Information for

'*Ab initio* optical study of graphene on hexagonal boron nitride and fluorographene substrates'

Xiao Lin, Yang Xu, Ayaz Ali Hakro, Tawfique Hasan, Ran Hao, Baile Zhang, and Hongsheng Chen

1. Optical conductivity of graphene double-layer structures

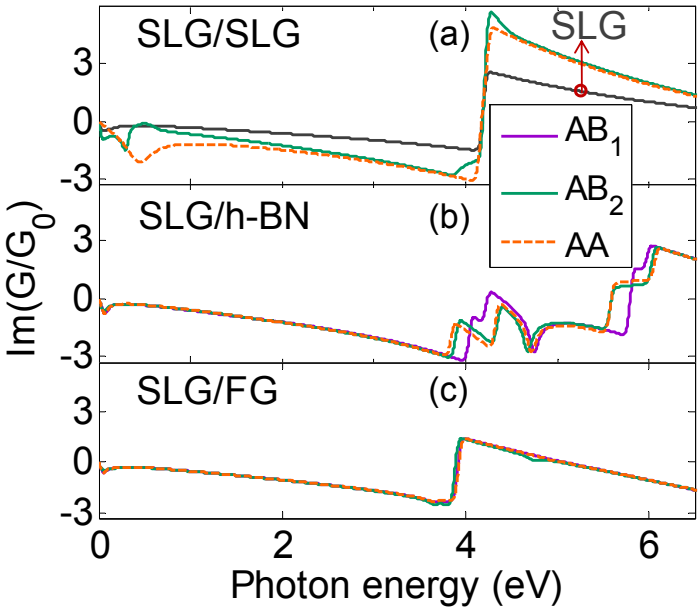

Figure S1: As a complete optical study of graphene double-layer structures in Fig. 2, the imaginary part of optical conductivity in a) SLG/SLG, b) SLG/*h*-BN, and c) SLG/FG are presented. The grey line is optical conductivity of SLG for reference. The optical properties of graphene on *h*-BN and FG substrates are both well preserved from near-infrared to visible frequencies, and the optical properties of graphene on FG substrate are much better preserved than that on *h*-BN substrate, especially at far-infrared and ultraviolet range.

2. Strain influence on optical properties of SLG, *h*-BN, and FG

Since the lattice mismatch of graphene is 5.7% with FG [45] and 1.5% with *h*-BN [39], through changing the bond length, the uniform in-plane strain influence on the optical properties of graphene, *h*-BN, and FG are investigated. The electronic and optical properties are firstly studied without strain in Fig. S2 and Fig. S3, respectively. In Fig. S2, graphene is zero-bandgap semiconductor with linear dispersion near the *K* point, whereas *h*-BN and FG are wide-bandgap semiconductors. In Fig. S3, the universality of optical conductivity of graphene exists below 1.0 eV, approximately in the visible region, and disappears in the ultraviolet region, which results agree with Ref. [1,2]. FG and *h*-BN have zero real part of optical conductivity below 3.7 eV and 4.5 eV, respectively, corresponding to zero light absorbance [47].

To fulfill the lattice match, the C-C bond in graphene (1.42 Å) is positively stretched (by +1.04%) to 1.435 Å in SLG/*h*-BN and (by +2.77%) to 1.459 Å in SLG/FG, the B-N bond in *h*-BN (1.45 Å) is compressed (by -1.05%) to 1.435 Å in SLG/*h*-BN, and the component of C-C bond parallel to the FG basal plane (1.501 Å) is negatively stretched (by -2.78%) to 1.459 Å in SLG/FG. In Fig. S3, the optical conductivity spectrum is only negatively correlated to strain in ultraviolet region. That we average the two lattice constants to commensurate the in-plane lattice mismatch of graphene, *h*-BN, and FG, therefore, would bring negligible changes on the optical conductivity and not alter the conclusions in the main text.

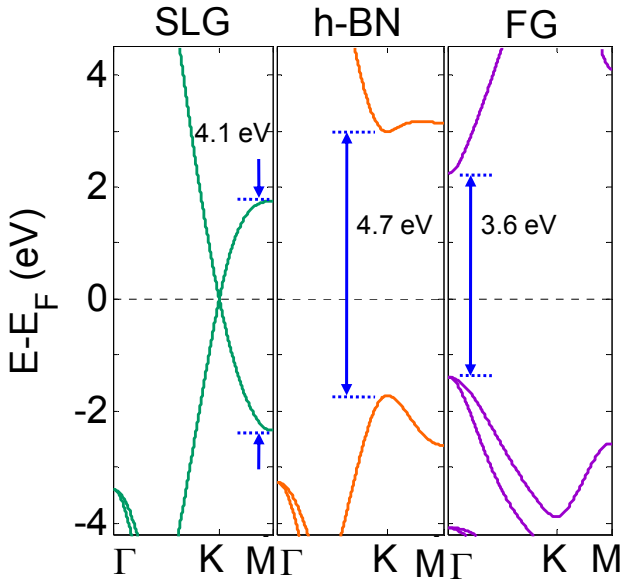

Figure S2: Band structures of SLG, *h*-BN, and FG. Our band structure calculation matches well with the results in Ref. [45,S1].

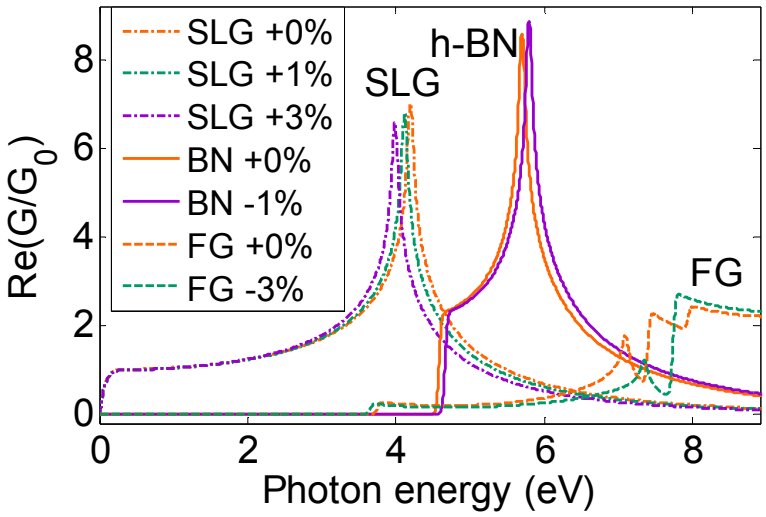

Figure S3: Strain (through changing the bond length) influence on the real part of optical conductivity in SLG, *h*-BN, and FG. The legend indicates the relative change of the bond length. The optical conductivities are found insensitive to the strain.

3. Structures of graphene double-layer structures

Graphene double-layer structure can be arranged in three typical stacking patterns as shown in the insets of Fig. 2, namely AB_1, AB_2, and AA. For AA stacking, each substrate atom is right below one graphene carbon atom. For AB stacking, half of substrate atoms are right below graphene carbon atoms, and the other half are beneath the graphene hexagonal centers. In SLG/SLG, AB_1 and AB_2 have identical configuration. In SLG/*h*-BN (SLG/FG), AB_1 stacking is characterized by each boron (fluorine) atom right below one carbon atom, whereas AB_2 stacking is characterized by each nitrogen (substrate carbon atom) atom right below one carbon atom. In SLG/SLG, the interlayer distance is 3.35 Å for energetically stable AB stacking [S2] and 3.55 Å for AA stacking [S3] from experiments, respectively. In SLG/*h*-BN, the interlayer distance is 3.22 Å for energetically stable AB_1 stacking, 3.40 Å for AB_2 stacking, and 3.50 Å for AA stacking from theoretical work [39], respectively. By calculating the total energy differences of SLG/FG with respect to freestanding graphene and FG as a function of interlayer distance, the equilibrium interlayer distances of SLG/FG can also be obtained by searching for the minimum total energy. The optimum inter-layer distances of SLG/FG (defined by the center of FG unit cell to the graphene plane) are 4.13 Å for AA, 4.12 Å for AB, and 3.94 Å for AB_2 stacking, respectively. In SLG/FG, AB_2 stacking has the minimum total energy, indicating AB_2 stacking is energetically stable. For simplicity, when calculating misalignment impact in Fig. 4, the double-layer structures are simulated with constant interlayer distance of their energetically stable structures.

4. Comparison of optical properties of graphene double-layer structures calculated by density functional theory and effective medium theory

In order to verify the interaction between graphene and the insulating 2D substrate, optical properties of SLG/SLG, SLG/*h*-BN, and SLG/CF calculated by density functional theory (DFT) and effective medium theory (EMT) are compared. In effective medium theory, since the interaction between graphene and substrate is ignored, the equivalent conductivity of graphene double-layer structure can be expressed as

$$\mathrm{Re(G)_{SLG/Substrate}} = [\mathrm{Re(G)_{SLG}} + \mathrm{Re(G)_{Substrate}}] \frac{\mathrm{d_{SLG/Substrate}}}{\mathrm{d_{SLG}} + \mathrm{d_{Substrate}}},$$

where *d* is the thickness. In Fig. S4, differences are found in conductivity spectrum at infrared and ultraviolet range calculated by two methods. For instance, in the optical conductivity spectrum of SLG/*h*-BN, the ultraviolet graphene peak is clearly split into two when calculated by DFT, while is well preserved when calculated by EMT. Hence, the interaction between graphene and substrate exists and has a strong influence on the optical properties of graphene.

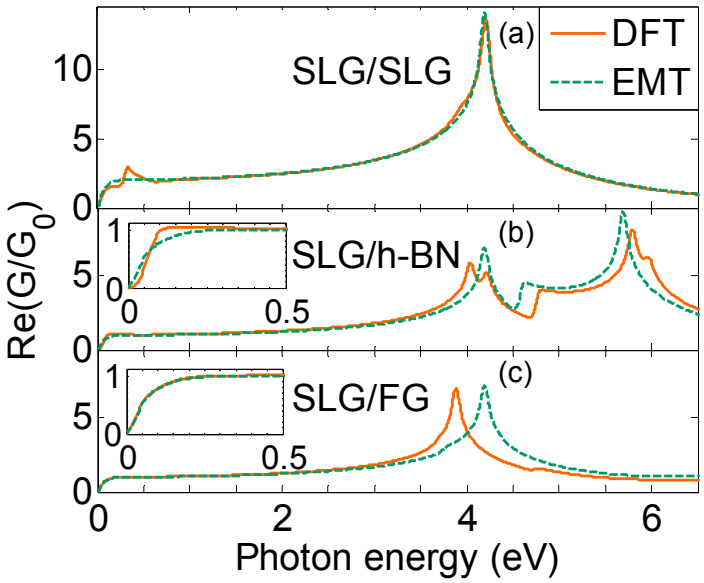

Figure S4: Optical conductivity comparison of energetically stable (a) AB stacking SLG/SLG, (b) AB_1 stacking SLG/*h*-BN, and (c) AB_2 stacking SLG/FG calculated by DFT (solid orange line) and EMT (dashed green line). The conductivity calculated by EMT is different from that by DFT, indicating the existence of interaction between graphene and substrate. For instance, in the optical conductivity spectrum of SLG/*h*-BN, the ultraviolet graphene peak is clearly split into two when calculated by DFT, while is well preserved when calculated by EMT. In AB_2 stacking SLG/FG, because the graphene Dirac point is well preserved, the optical properties calculated by DFT and EMT are the same below 0.5 eV as shown in the inset of (c).

5. Misalignment-dependent optical properties of graphene double-layer structures

To clearly present the influence of misalignment on optical properties of graphene double-layer structures, Fig. 4 is re-drawn to the plane of photon energy vs. optical conductivity in Fig. S5. As a complete investigation of Fig. 4, the influence of misalignment along the y direction on the optical conductivity of graphene double-layer structures is shown in Fig. S6.

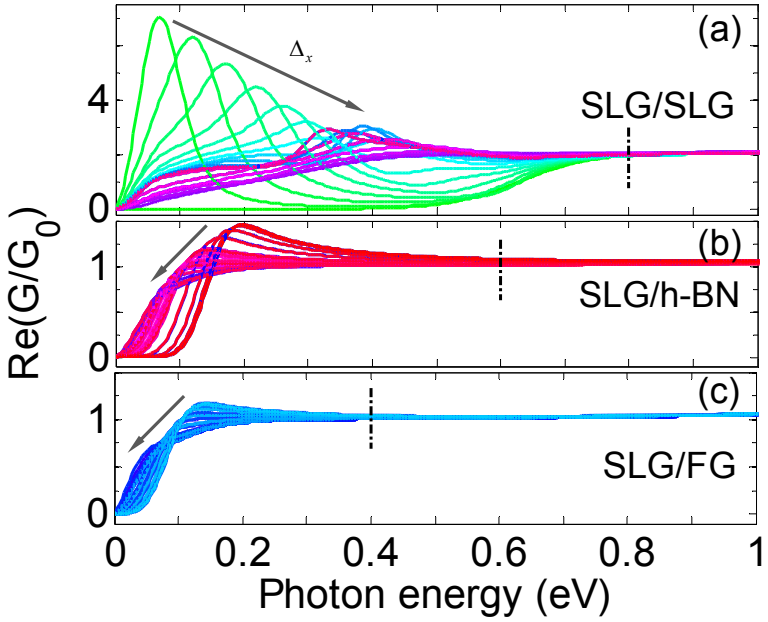

Figure S5: Influence of misalignment on optical conductivity in graphene double-layer structures. The black arrows indicate the change of misalignment vector along the *x* direction Δ_x from 0 to 3 times of graphene bond length in Fig. 4. Optical conductivity is sensitive to misalignment below 0.8 eV in SLG/SLG, below 0.6 eV in SLG/*h*-BN, and below 0.4 eV in SLG/FG, respectively, where relative conductivity change (defined as $(Re(G)_{max}-Re(G)_{min})/Re(G)_{min}$) is >5%.

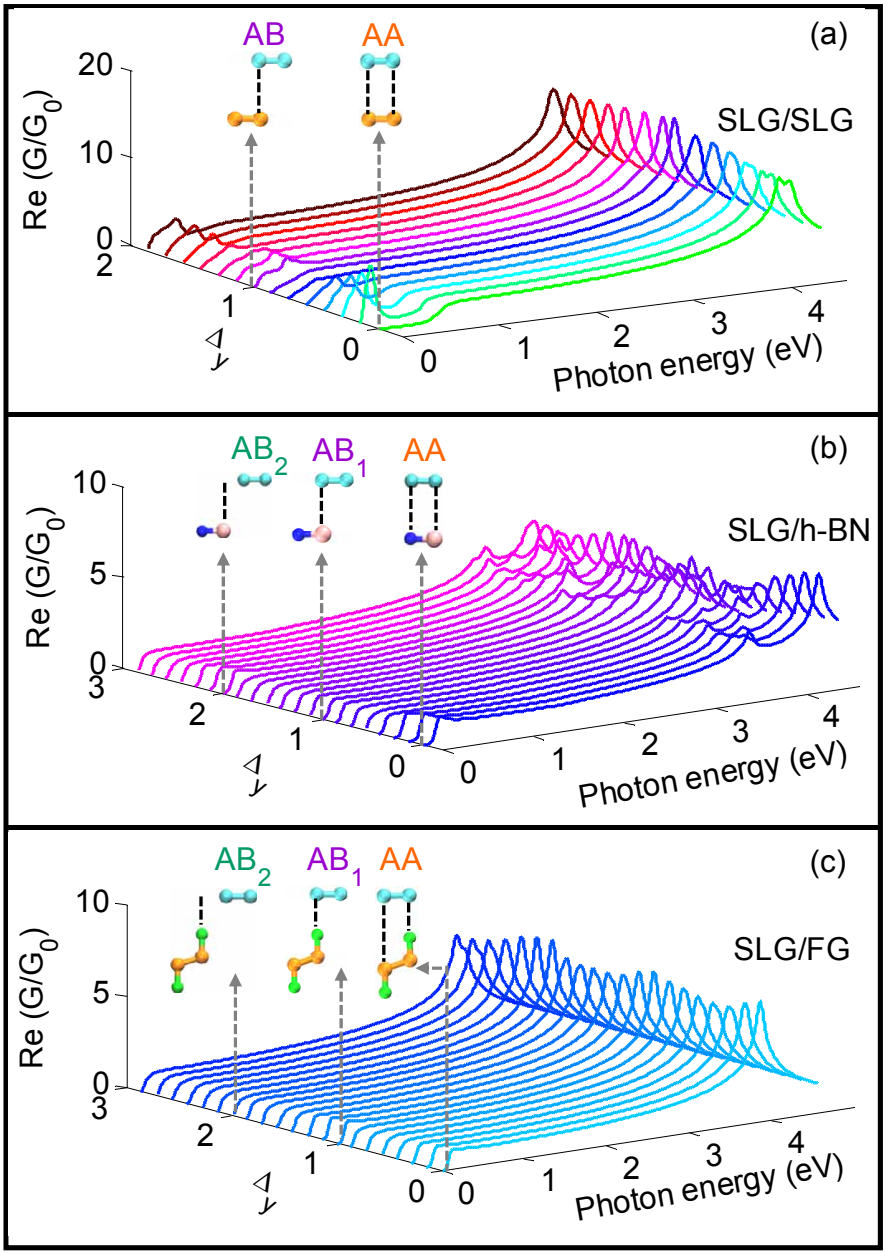

Figure S6: Influence of misalignment on optical conductivity of AA, AB_1, and AB_2 stacking graphene double-layer structures. Δ_y is the misalignment vector along the *y* direction normalized by graphene bond length. For clarity, relative misalignments in AA, AB_1, and AB_2 are denoted by 0, 1, and 2 in Δ_y, respectively. Optical properties of graphene heterostructures have a strong dependence on misalignment, in particular at frequencies <0.4 eV or >3.5 eV.

6. Optical properties of doped SLG and SLG/*h*-BN

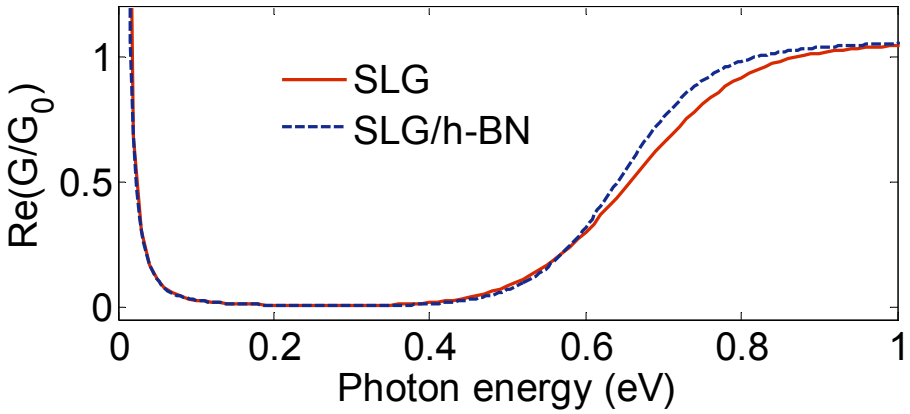

Figure S7: Optical conductivity of SLG and SLG/*h*-BN with 0.29 eV chemical potential. The complex optical conductivity used in Fig. 8 is $G = G_{\text{inter}} + G_{\text{intra}}$, where G_{inter} is calculated by density functional theory and G_{intra} is calculated by Kubo formula. Since the DC mobility of $\mu > 100{,}000\, cm^2 V^{-1} s^{-1}$ [28] has been experimentally achieved in high-quality suspended graphene and $\mu > 60{,}000\, cm^2 V^{-1} s^{-1}$ [35] in graphene on *h*-BN substrate, the choice of $\tau = 0.9\, ps$ here is rather conservative in the calculation of G_{intra} in both graphene and SLG/*h*-BN due to $\tau = \mu_c \mu / (e v_F^2)$ [28]. Because chemical potential is far above 0.2 eV, Re(G) at 0.1 eV (and 0.2 eV) is mainly caused by the intra-band and non-vertical inter-band transitions, leading to Re(G)s of graphene and SLG/*h*-BN at 0.1 eV (and 0.2 eV) almost the same. Therefore, in Figs. 8(d,f,h), the substrate influence on the ON state of the surface plasmonic modulator is negligible.

7. The influence of a substrate defect on graphene optical properties

A defect on substrate is a very important issue from the experimental view. Real substrates could have a number of defects in the crystal structure, which may include both impurity atoms and irregularities in the alignment of atoms. Defects can be classified as being either point defects or linear defects. For point defects, the simplest type is formed when atoms are missing from the lattice, known as vacancies. Linear defects occur when a crystal structure contains misaligned planes of atoms. Due to the limited computing ability, we choose the vacancy defect on *h*-BN substrate to study the influence on graphene optical properties, which needs fewer atom number in the calculating unit cell. For a purely theoretical study in Fig.S8, a B or N atom is missing in the unit cell of C_4/B_2N_2 and C_8/B_4N_4 in energetically stable AB_1 stacking SLG/*h*-BN. Due to computational limitation, we have to point out that the vacancy in our simulation is very different from realistic situation in experiments and our introduced artificial vacancy density is much larger than that in experiments. In the "Calculation Methods" section, in order to accelerate the calculation, the Gaussian broaden increases from 0.04 eV to 0.08 eV and the photon energy range decreases from 0-40 eV to 0-4.5 eV. In Fig.S8, the graphene optical properties change radically as defects appear in *h*-BN substrate, especially below 2 eV. The B vacancy and N vacancy have different influence on the graphene optical properties. In SLG/*h*-BN, the p_z orbitals of sp^2 hybridized boron and nitrogen atoms in *h*-BN might be partially overlapped with the neighbouring p_z orbitals of sp^2 hybridized carbon atoms in graphene. Thus, the B or N vacancies in SLG/*h*-BN may cause the change of local carrier density of states in graphene spectrum. In Fig.S8, the peak absorption below 0.5 eV photon energy may be due to the increase of the local carrier density of states in graphene while the absorption reduction from

~0.5 eV to ~1.5 eV may be caused by the decrease of the local carrier density of states. Meanwhile in SLG/*h*-BN, the electron/hole transition may happen from valence bands to conduction bands not only in the same layer but also between adjacent layers. The dip and peak absorptions above 1.5 eV might be due to electron/hole transitions between graphene layer and defected *h*-BN layer. Thus we argue that the small substrate vacancy defect density in reality will at least have a strong influence on the local optical properties of graphene. Our results show that the defects in sample should be carefully treated.

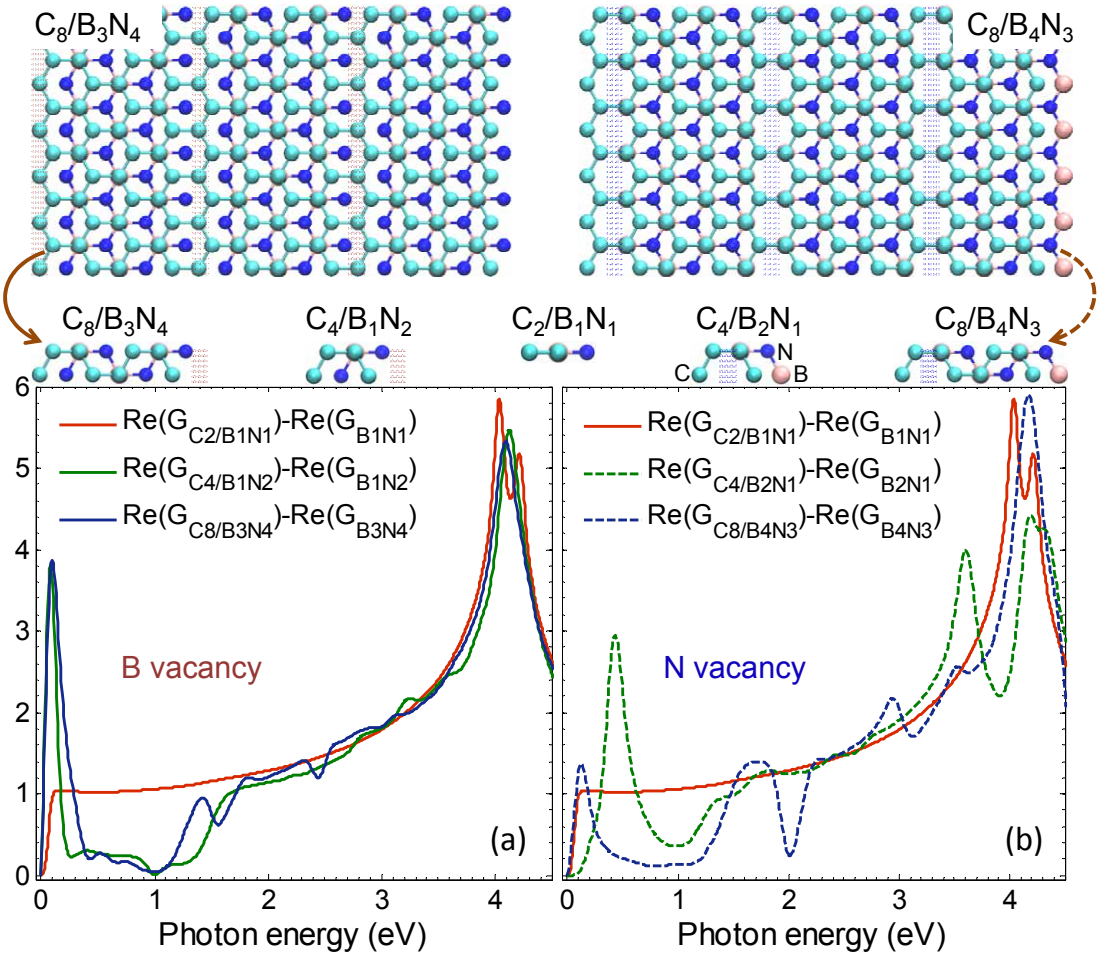

Figure S8: Influence of *h*-BN substrate vacancy defects on graphene optical conductivity (real part, Re(G), in unit of G_0). (a) A boron atom vacancy is artificially introduced in the unit cell of C_4/B_2N_2 (namely C_4/B_1N_2, green solid line) and C_8/B_4N_4 (C_8/B_3N_4, blue solid line) in energetically stable AB_1 stacking SLG/*h*-BN. (b) A nitrogen atom vacancy is artificially introduced in the unit cell of C_4/B_2N_2 (C_4/B_2N_1, green dashed line) and C_8/B_4N_4 (C_8/B_4N_3, blue dashed line) in SLG/*h*-BN. A boron (nitrogen) atom vacancy in C_8/B_4N_4 are schematically shown in the top left (top right), where the shadow regions indicate the location of missing atoms. The unit cells in our simulation are given in the middle. As a reference, the intact SLG/*h*-BN with C_2/B_1N_1 unit cell (no defects, red solid line) is also shown.

8. The influence of a substrate size on graphene optical properties

When the substrate (for instance *h*-BN) is much larger than graphene, from the point of tight-binding theory, every C atom in graphene will mainly interact with the nearby B or N atoms in *h*-BN substrate. Since there are dangling bonds at the graphene boundary, we argue that graphene may be divided into two regions as shown in Fig.S9(a): The 1st part far away from the graphene boundary can be treated as homogeneous SLG/*h*-BN heterostructure, and the 2nd part near the graphene boundary should be different from 1st part and have a strong dependence on the properties of graphene boundary supported by *h*-BN substrate. When the graphene flake is large enough, the atoms at the boundary will only have a small percentage and then the region of graphene supported by a much larger *h*-BN substrate may be treated as homogeneous SLG/*h*-BN heterostructure. Since the two parts in Fig.S9(a) are both far away from the *h*-BN boundary, we argue that the *h*-BN substrate boundary has trivial impact on graphene optical properties and there should be no size dependent on the *h*-BN substrate size. When the *h*-BN substrate is a bit smaller than graphene, C atoms in graphene close to the boundary of the *h*-BN substrate may interact with the B or N atoms, but are strongly dependent on the local atomic environments. Hence, graphene can not be treated as homogeneous. When the *h*-BN substrate is smaller than graphene, we argue that graphene can be divided into at least three regions as shown in Fig.S9(b): the 1st part of graphene supported by *h*-BN substrate far away from the *h*-BN substrate boundary may be treated as homogeneous SLG/*h*-BN heterostructure, the 2nd part of graphene near the *h*-BN substrate boundary should be strongly affected by the *h*-BN boundary, and the 3rd part of graphene far away from the *h*-BN substrate may be treated as freestanding graphene. In the 8th section, we have investigated the influence of a substrate defect on graphene optical properties, where the defect density is large. When the vacancy defect density is large enough (for instance, a B or N atom is missing in the unit cell of (C_8/B_4N_4) in AB_1 stacking SLG/*h*-BN), the vacancies in Fig.S8 might behave similar to the boundary of *h*-BN substrate in Fig.S9(b) with width

smaller than graphene. From the results in the 8th section, we can conclude that the optical properties of the 2nd part graphene affected by the *h*-BN substrate boundary should be quite different from freestanding graphene and SLG/*h*-BN heterostructure. The percentages of the three parts will vary when the size of *h*-BN substrate changes. In this case, we argue that when the substrate is a bit smaller than the graphene, there may be size dependent.

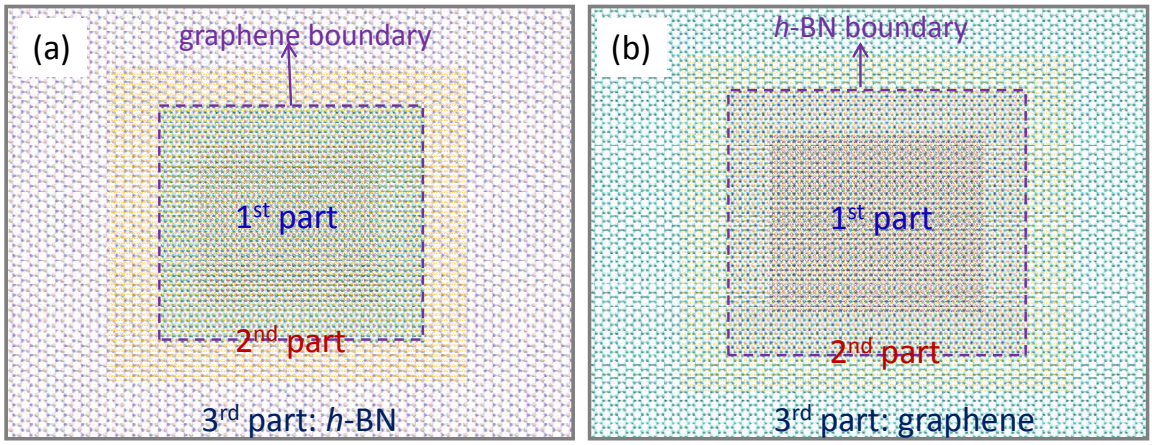

Figure S9: Schematics of graphene on *h*-BN substrate. (a) The *h*-BN substrate is much larger than graphene. We argue that graphene may be divided into two regions: The 1st part far away from the graphene boundary can be treated as homogeneous SLG/*h*-BN heterostructure, and the 2nd part near the graphene boundary should be different from 1st part and strongly affected by the graphene boundary. (b) The *h*-BN substrate is smaller than graphene. We argue that graphene can be divided into three regions: the 1st part supported by *h*-BN substrate far away from the *h*-BN substrate boundary may be treated as homogeneous SLG/*h*-BN heterostructure, the 3rd part far away from the *h*-BN substrate may be treated as freestanding graphene, and the 2nd part near the *h*-BN substrate boundary affected by the *h*-BN boundary should be different from 1st part and 3rd part.

Supporting References

[S1] H. Şahin, S. Cahangirov, M. Topsakal, E. Bekaroglu, E. Akturk, R. T. Senger, S. Ciraci, *Phys. Rev. B*, 2009, **80**, 155453.

[S2] M. Hanfland, H. Beister, K. Syassen, *Phys. Rev. B*, 1989, **39**, 12598-12603.

[S3] J. K. Lee, S. C. Lee, J. P. Ahn, S. C. Kim, J. I. B. Wilson, P. John, *J. Chem. Phys.*, 2008, **129**, 234709.